Complex Systems Stability & Control
https://www.sciltp.com/journals/cssc

Check for updates

Article

Anti-Disturbance Dynamic Memory Event-Triggered Control for Robotic Manipulator Systems

Pengfei Zhang [1], Ying Zhao [1,*], Changyi Xu [2] and Chao Zhang [3]

[1] College of Marine Electrical Engineering, Dalian Maritime University, Dalian 116026, China
[2] The College of Control Science and Engineering, Dalian University of Technology, Dalian 116024, China
[3] The College of Mechanical Engineering, Zhejiang University, Hangzhou 310030, China
* Correspondence: yingz@dlmu.edu.cn

How To Cite: Zhang, P.; Zhao, Y.; Xu, C.; et al. Anti-Disturbance Dynamic Memory Event-Triggered Control for Robotic Manipulator Systems. *Complex Systems Stability & Control* **2026**, *2*(3), 11. https://doi.org/10.53941/cssc.2026.100022

Received: 13 April 2026
Revised: 6 May 2026
Accepted: 6 May 2026
Published: 10 August 2026

Abstract: This study investigates the H_∞ anti-disturbance dynamic memory event-triggered (ADDMET) control issue for Robotic Manipulator System (RMS) under multiple disturbances. An affine model is adopted to characterize the RMS, accounting for payload variations and complex operating conditions. An observer is designed to estimate and compensate for disturbances caused by modeling uncertainties and external perturbations. Based on the proposed observer, a dynamic memory event-triggered mechanism (DMETM) and an H_∞ anti-disturbance event-triggered controller are developed. This conserves communication resources and reduces control effort. Sufficient conditions for the solvability of the H_∞ ADDMET control problem are derived. Finally, a numerical simulation is established based on the affine model to validate the effectiveness of the proposed method.

Keywords: robotic manipulator system; affine models; anti-disturbance; dynamic memory event-triggered control

1. Introduction

With the rapid development of intelligent manufacturing and robotic technologies, networked and intelligent control strategies have been increasingly applied to robotic manipulator systems (RMSs) [1]. The dynamic behavior of robotic manipulators is inherently nonlinear and subject to various physical constraints. In practical applications, RMSs are required to simultaneously satisfy multiple performance requirements [2, 3], including steady-state accuracy, transient response, and operational safety. It poses significant challenges to modeling and control design [4]. In recent years, a variety of modeling approaches have been developed for RMSs, achieving notable progress [5–7].

To more accurately capture varying equilibrium points and complex operating conditions, affine systems (ASs) have been introduced [8, 9]. Compared with conventional linearized systems, ASs incorporate additional affine terms, allowing the model to explicitly account for equilibrium point shifts [10, 11]. This feature enables a more precise characterization of performance degradation, payload changes, and configuration variations. When the affine terms vanish, the AS reduces to a standard linear system. The existence of these affine terms reflects the physical reality that the system's actual equilibrium point may deviate from the nominal one due to uncertainties or operational constraints, making it essential to properly determine and regulate the desired operating point [12–14].

In practical scenarios, robotic manipulators are often affected by performance degradation, payload variations, and manufacturing uncertainties, which may cause shifts in equilibrium points and consequently degrade system performance [15, 16]. In multi-joint manipulators, such deviations may even lead to critical issues, such as end-effector positioning errors induced by joint torque mismatch [17]. Therefore, it is essential for RMSs to accommodate these variations in operating characteristics. The affine modeling framework provides an effective means to describe such behaviors, especially for systems subject to long-term operation, component aging, and configuration-dependent nonlinearities.

Moreover, RMSs are inevitably influenced by various disturbances, including both modeled and unmodeled disturbances [18]. Modeled disturbances typically arise from measurable factors such as payload changes and external interactions, while unmodeled disturbances are caused by system uncertainties, unmodeled dynamics, and environmental perturbations [19,20]. These disturbances can significantly degrade control performance and even destabilize the system. Hence, anti-disturbance (AD) control has become a critical issue in robotic manipulator systems. Existing AD strategies often rely on disturbance observers or internal model-based approaches to estimate and compensate for disturbances, thereby improving system robustness [21].

In addition, with the rapid advancement of networked control technologies, event-triggered (ET) control schemes have been widely adopted in RMSs to reduce communication and computational burdens while maintaining desired performance [22]. ET-based anti-disturbance control methods have also been developed to enhance robustness under disturbance conditions [23,24]. The dynamic event-triggered (DET) mechanism further improves resource utilization by introducing internal dynamic variables [25]. Recently, the dynamic memory event-triggered mechanism (DMETM) has been proposed, which incorporates historical information into the triggered condition to reduce unnecessary transmissions while preserving system stability [26]. However, the application of DMETM to RMSs has not yet been fully investigated. By leveraging memory information, DMETM can effectively reduce communication load and improve control performance, making it particularly suitable for resource-constrained robotic systems.

Motivated by the above discussions, this study investigates the H_∞ anti-disturbance dynamic memory event-triggered control problem for RMSs modeled by affine systems. The main contributions are summarized as follows: First, a novel H_∞ anti-disturbance dynamic memory event-triggered (ADDMET) control framework is proposed for robotic manipulator systems (RMSs). This framework utilizes an affine modeling approach to explicitly capture equilibrium point shifts caused by payload variations and complex operating conditions. Second, a dynamic memory event-triggered mechanism (DMETM) is developed. Compared to existing static [22,27] and dynamic [28,29] event-triggered schemes, the proposed DMETM significantly reduces the triggered frequency. It achieves this by utilizing historical triggered information to adaptively adjust the execution threshold. Finally, an integrated disturbance observer is designed to effectively estimate and compensate for multiple external disturbances. Consequently, the proposed scheme rigorously guarantees the desired H_∞ performance and asymptotic stability while successfully excluding Zeno behavior.

The structure is summarized as follows. In Section 2, the description of the RMS modeled as ASs is introduced. In Section 3, the H_∞ ADDMET control scheme of this study is introduced. In Section 4, the simulation of the RMS is developed. In Section 5, we provide the conclusions.

The notations are summarized as Table 1.

Table 1. Symbols.

Notation	Meaning
$\mathfrak{N}$	Non-negative integers collection
R^{n*n}	Real space of $n*n$-dimensional
$L_2[0,\infty)$	Space of squared integrable functions on $[0,\infty)$
$diag\{X\}$	Diagonal matrix
I	Identity matrix
x^φ	Desired EP
X^T	Transpose
$X(\varphi)$	Convex combination
$\|\|X\|\|$	Two-norm
λ_{max}(X)	The largest eigenvalue
λ_{min}(X)	The smallest eigenvalue

2. Problem Formulation

2.1. System Introduction and Observer Construction

For a two–degree–of–freedom robotic manipulator, the dynamics can be expressed as

$$M(q)\ddot{q}(t) + C(q,\dot{q})\dot{q}(t) + G(q) = \tau(t) + d(t), \tag{1}$$

where $q(t) = [q_1(t), q_2(t)]^T \in R^{2\times 1}$ denotes the joint angle vector, $\dot{q}(t)$ and $\ddot{q}(t)$ represent the joint velocity and acceleration vectors, respectively. $M(q) \in R^{2\times 2}$ is the inertia matrix, $C(q,\dot{q}) \in R^{2\times 2}$ represents the Coriolis and centrifugal matrix, $G(q) \in R^{2\times 1}$ denotes the gravity term, $\tau(t) \in R^{2\times 1}$ is the control torque input, and $d(t) \in R^{2\times 1}$ represents external disturbances.

Due to nonlinear coupling and varying operating configurations, the manipulator dynamics are usually linearized around several equilibrium points. Applying local linearization around the equilibrium point leads to the following first-order approximation

$$\Delta\dot{q}(t) = F\Delta q(t) + G\Delta\tau(t) + b, \tag{2}$$

where F and G denote the system and input matrices and b represents the equilibrium shift caused by modeling uncertainties or payload variations.

The affine model of the robotic manipulator system at the given equilibrium point p can be obtained via local linearization and system identification as

$$\begin{aligned} \begin{bmatrix} \Delta\dot{q}_1(t) \\ \Delta\dot{q}_2(t) \end{bmatrix} &= F \begin{bmatrix} \Delta q_1(t) \\ \Delta q_2(t) \end{bmatrix} + G\Delta\tau(t) + b, \\ \Delta y(t) &= H \begin{bmatrix} \Delta q_1(t) \\ \Delta q_2(t) \end{bmatrix}, \end{aligned} \tag{3}$$

where $F \in R^{n_x\times n_x}$, $G \in R^{n_u\times 1}$ and $H \in R^{2\times n_z}$, represent the system matrix, control input matrix and output matrix of the robotic manipulator system, respectively. b represents the equilibrium-point shift term caused by variations such as payload changes, modeling uncertainties, or configuration-dependent nonlinear effects in the robotic manipulator.

The relevant signs are listed as Table 2.

Table 2. Nomenclature.

Notation	Meaning
$q_1(t)$	Actual joint 1 angle
$q_2(t)$	Actual joint 2 angle
$\tau(t)$	Control torque input
$q_1^p(t)$	Joint 1 angle at equilibrium point
$q_2^p(t)$	Joint 2 angle at equilibrium point
$\tau^p(t)$	Torque at equilibrium point
$\Delta q_1(t)$	Joint 1 angle increment $q_1(t) - q_1^p(t)$
$\Delta q_2(t)$	Joint 2 angle increment $q_2(t) - q_2^p(t)$
$\Delta\tau(t)$	Torque increment $\tau(t) - \tau^p(t)$
$\Delta y(t)$	Output increment
b	Equilibrium shift term

Consider the RMS with the modeled disturbance $\xi_1(t)$ and unmodeled disturbance $\xi_2(t)$, described as

$$\begin{aligned} \begin{bmatrix} \Delta\dot{q}_1(t) \\ \Delta\dot{q}_2(t) \end{bmatrix} &= F \begin{bmatrix} \Delta q_1(t) \\ \Delta q_2(t) \end{bmatrix} + G[\Delta\tau(t) + \xi_1(t)] + E\xi_2(t) + b, \\ \Delta y(t) &= H \begin{bmatrix} \Delta q_1(t) \\ \Delta q_2(t) \end{bmatrix}, \end{aligned} \tag{4}$$

and $\xi_1(t)$ acts as the exo-system output

$$\begin{aligned} \dot{\theta}(t) &= A\theta(t) + B\xi_3(t), \\ \xi_1(t) &= C\theta(t), \end{aligned} \tag{5}$$

where $\theta(t)$ standing for the exo-system state and unmodeled disturbance $\xi_2(t), \xi_3(t) \in L_2\,[0,\infty)$.

Letting $x(t) = [\Delta q_1^T(t)\ \ \Delta q_2^T(t)]^T$ and $u(t) = \Delta\tau(t)$, the robotic manipulator system (4) is formulated as an affine system

$$\begin{aligned} \dot{x}(t) &= Fx(t) + G[u(t) + \xi_1(t)] + E\xi_2(t) + b, \\ z(t) &= Hx(t), \end{aligned} \tag{6}$$

where $x(t) \in R^{n_x \times 1}$, $u(t) \in R^{n_u \times 1}$ and $z(t) \in R^{n_z \times 1}$ represent the state, control input and output of the robotic manipulator system, respectively.

Note that the desired EP x^{φ} may not coincide with the current system equilibrium point and usually belongs to the group $X^{\varphi} = \{x^{\varphi} \in R^{n_{x^{\varphi}} \times 1} \mid A(\varphi)x^{\varphi} + b(\varphi) = 0\}$.

By setting $x_{\varphi}(t) = x(t) - x^{\varphi}$, the error dynamics can be obtained as

$$\begin{aligned} \dot{x}_{\varphi}(t) &= Fx_{\varphi}(t) + G[u(t) + \xi_1(t)] \\ &\quad + E\xi_2(t) + l, \\ z_{\varphi}(t) &= Hx_{\varphi}(t), \end{aligned} \tag{7}$$

where $l = Fx^{\varphi} + b$ is the AT, and $z_{\varphi}(t) = z(t) - Hx^{\varphi}$, represent the output that is converted to the origin.

Based on the AS (6) of the RMS (4), we formulate the control issue of this paper.

Firstly, to compensate for the effects induced by the disturbance $\xi_1(t)$ on the RMS (6), we establish the sliding window disturbance observer

$$\begin{aligned} &\dot{\beta}(t) = (A + \Lambda GC)[\beta(t) - \Lambda x_{\varphi}(t)] + \Lambda[Fx_{\varphi}(t) + Gu(t)] + \sum_{n=1}^{N} \tilde{z}_{\varphi}(t - n\tau), \\ &\hat{\theta}_{\varphi}(t) = \beta(t) - \Lambda x_{\varphi}(t), \\ &\hat{\xi}_1(t) = C\hat{\theta}_{\varphi}(t), \end{aligned} \tag{8}$$

where $\hat{\xi}_1(t)$ and $\hat{\theta}_{\varphi}(t)$ represent the estimation $\xi_1(t)$ and $\theta_{\varphi}(t)$, respectively. $\tau > 0$ is a constant denoting the sliding interval, and Λ represents the gain of the sliding window disturbance observer to be determined. The parameter N denotes the size of the sliding window in the observer design, specifying the number of past samples of the output estimation error.

Secondly, for the purpose of communication resource optimization of the RMS (4), the following DMETM is considered

$$t_{\mathfrak{s}+1} = inf\{t > t_{\mathfrak{s}} \mid \eta(t) + \iota(\sigma\tilde{x}^T(t)I_1\tilde{x}(t) - v^T(t)I_2v(t)) \leq 0\}, \mathfrak{s} \in \mathfrak{N} \tag{9}$$

where $\mathfrak{s}$ stands for the number of triggers, the state error $v(t) = x_{\varphi}(t_{\mathfrak{s}}) - x_{\varphi}(t), t \in [t_{\mathfrak{s}}, t_{\mathfrak{s}+1}), \iota, \sigma > 0$, $I_1, I_2, I_3 > 0$ and $\eta(t)$ is the dynamic variable that satisfies

$$\begin{cases} \dot{\eta}(t) = -\kappa\eta(t) + \iota(\sigma\tilde{x}^T(t)I_1\tilde{x}(t) - v^T(t)I_2v(t)) + me^{-m(t-n\tau)} \sum_{n=1}^{N} \tilde{z}_{\varphi}^T(t - n\tau)I_3\tilde{z}_{\varphi}(t - n\tau), \\ \eta(0) = \eta_0, \end{cases} \tag{10}$$

where $\kappa > 0, m > 0, \eta(0) > 0, \mathfrak{s} \in \mathfrak{N}$.

Remark 1. *In contrast to the usual static ET rules [22, 27] and DET [28, 29], (9) includes the output $\tilde{z}_{\varphi}(t)$ and its memory. This conserves the transmission resources from the RMS (4) to controller $u(t)$, reducing the fuel consumption.*

Then, a state-dependent controller is built as

$$u(t) = -\hat{\xi}_1(t) + Lx_{\varphi}(t_{\mathfrak{s}}), \tag{11}$$

where L is the controller gain that need to be arranged.

By defining $e(t) = \theta_{\varphi}(t) - \hat{\theta}_{\varphi}(t)$, the error system can be derived as

$$\dot{e}(t) = (A + \Lambda GC)\, e(t) + \Lambda E\xi_2(t) + B\xi_3(t) - \sum_{n=1}^{N} \tilde{z}_{\varphi}(t - n\tau) + \Lambda l_{r(t)} \tag{12}$$

Substituting (11) into (7) generates that

$$\begin{aligned} \dot{x}_{\varphi}(t) &= (F + GL)\, x_{\varphi}(t) + GCe(t) + E\xi_2(t) + GLv(t) + l \\ z_{\varphi}(t) &= Hx_{\varphi}(t) \end{aligned} \tag{13}$$

Combining (12) and (13), the augmented system is developed by

$$\begin{aligned}\dot{\tilde{x}}(t) &= \tilde{A}\tilde{x}(t) + \tilde{B}\tilde{\xi}(t) + \tilde{D}\sum_{n=1}^{N}\tilde{z}(t-n\tau) + L^f + \tilde{E}v(t) \\ \tilde{z}(t) &= \tilde{H}\tilde{x}(t)\end{aligned} \tag{14}$$

where $\tilde{x}(t) = [x_\varphi^T(t)\ \ e^T(t)]^T, \tilde{\xi}(t) = [\xi_2^T(t)\ \ \xi_3^T(t)]^T$,

$$\tilde{A}_i = \begin{bmatrix} F+GL & GC \\ 0 & A+\Lambda GC \end{bmatrix}, \tilde{B} = \begin{bmatrix} E & 0 \\ \Lambda E & B \end{bmatrix}, \tilde{D} = \begin{bmatrix} 0 \\ -I \end{bmatrix}, L^f = \begin{bmatrix} l \\ \Lambda l \end{bmatrix},$$
$$\tilde{E} = \begin{bmatrix} GL \\ 0 \end{bmatrix}, \quad \tilde{H} = \begin{bmatrix} H & 0 \\ * & 0 \end{bmatrix}.$$

Next, based on the augmented system (14), the problem of H_∞ ADDMET control is described.

Definition 1. *Ref. [30] Consider the AS (6). Assume that there exists the disturbance observer (8), DMETM (9), controller (11), such that the following H_∞ ADDMET property is driven:*

- **(i)** *When $\tilde{\xi}^T(t) \equiv 0$, the system (14) exhibits asymptotical stability.*
- **(ii)** *When $\tilde{\xi}^T(t) \neq 0$, under the zero initial, for a given scalar β, the L_2-gain performance*

$$\int_0^\infty z^T(t)z(t)dt \leq \beta^2 \int_0^\infty \tilde{\xi}^T(t)\tilde{\xi}(t)dt \tag{15}$$

is held, the given constant $\beta > 0$ is called the L_2-gain level. Then, the H_∞ ADDMET control issue of the RMS (4) is solvable. The disturbance observer (8), DMETM (9) and controller (11) are called the H_∞ ADDMET control approach.

3. Analysis and Design

The H_∞ ADDMET property is analysed in this section. The disturbance observer (8), DMETM (9) and controller (11) are co-built to solve the H_∞ ADDMET control issue.

First, to ensure the solvability of the H_∞ ADDMET control problem, a criterion is provided.

Theorem 1. *For the AS (6) with given positive constants σ, if there exists a strictly positive definite symmetric matrix P, such that the constraints*

$$\Upsilon = \begin{bmatrix} \Lambda & P\tilde{B} & P\tilde{E} \\ * & -\beta^2 I & 0 \\ * & * & -I_2 \end{bmatrix} < 0, \tag{16}$$

hold, where

$$\Lambda = P\tilde{A} + \tilde{A}^T P + \sigma I_1 + \left(\sum_{n=1}^{N} e^{-mn\tau} + 1\right)\tilde{H}^T\tilde{H} - R + 3P\tilde{D}\tilde{D}^T P^T,$$

$$P = \text{diag}\{P_1, P_2\} \quad P > 0, P_1, P_2 \in R^{2\times 2}$$

the sliding window disturbance observer (8), DMETM (9) and controller (11), the augmented system (14) ensures the H_∞ ADDMET property.

Proof. Select the Lyapunov function

$$W(\tilde{x}_\varphi(t)) = \tilde{x}^T(t)P\tilde{x}(t) + \eta(t) + \sum_{n=1}^{N}\int_{t-n\tau}^{t} e^{-m\varepsilon}\tilde{z}_\varphi^T(\varepsilon)T\tilde{z}_\varphi(\varepsilon)d\varepsilon \tag{17}$$

Differentiating the Lyapunov function (17) in the triggered interval $[t_{\mathfrak{s}}, t_{\mathfrak{s}+1}), \mathfrak{s} \in \mathfrak{N}$ produces

$$\begin{aligned}
&\dot{W}(\tilde{x}_\varphi(t)) \\
&= 2\tilde{x}^T(t)P\dot{\tilde{x}}(t) - k\eta(t) + \sigma\tilde{x}^T(t)I_1\tilde{x}(t) - v^T(t)I_2v(t) - m\sum \tilde{z}_\varphi^T(t-n\tau)I_3\tilde{z}_\varphi(t-n\tau) \\
&\quad + \sum_{n=1}^{N} e^{-mn\tau}\tilde{z}_\varphi^T(t)T\tilde{z}_\varphi(t) - \sum_{n=1}^{N} e^{-m(t-n\tau)}\tilde{z}_\varphi^T(t-n\tau)T\tilde{z}_\varphi(t-n\tau) \\
&= \tilde{x}^T(t)\left(P\tilde{A} + \tilde{A}^TP + \sigma I_1\right)\tilde{x}(t) + 2\tilde{x}^T(t)P\tilde{D}\sum_{n=1}^{N}\tilde{z}(t-n\tau) + 2\tilde{x}^T(t)PL^f \\
&\quad + 2\tilde{x}^T(t)P\tilde{E}v(t) - k\eta(t) - v^T(t)I_2v(t) - m\sum_{n=1}^{N}\tilde{z}_\varphi^T(t-n\tau)I_3\tilde{z}_\varphi(t-n\tau) \\
&\quad + \sum_{n=1}^{N} e^{-mn\tau}\tilde{z}_\varphi^T(t)T\tilde{z}_\varphi(t) + 2\tilde{x}^T(t)P\tilde{B}\tilde{\xi}(t)
\end{aligned} \tag{18}$$

it follows that:

$$\begin{aligned}
&\dot{W}(\tilde{x}(t)) + \tilde{z}^T(t)\tilde{z}(t) - \beta^2\tilde{\xi}^T(t)\tilde{\xi}(t) \\
&= \dot{W}(\tilde{x}(t)) + \tilde{x}^T(t)\tilde{H}^T\tilde{H}\tilde{x}(t) - \beta^2\tilde{\xi}^T(t)\tilde{\xi}(t) \\
&= \tilde{x}^T(t)\left(P\tilde{A} + \tilde{A}^TP + \sigma I_1 + \tilde{H}^T\tilde{H}\right)\tilde{x}(t) + 2\tilde{x}^T(t)P\tilde{B}\tilde{\xi}(t) + 2\tilde{x}^T(t)P\tilde{D}\sum_{n=1}^{N}\tilde{z}(t-n\tau) \\
&\quad + 2\tilde{x}^T(t)PL^f + 2\tilde{x}^T(t)P\tilde{E}v(t) - m\sum_{n=1}^{N}\tilde{z}_\varphi^T(t-n\tau)I_3\tilde{z}_\varphi(t-n\tau) - \beta^2\tilde{\xi}^T(t)\tilde{\xi}(t) \\
&\quad - \sum_{n=1}^{N} e^{-m(t-n\tau)}\tilde{z}_\varphi^T(t-n\tau)T\tilde{z}_\varphi(t-n\tau) + \sum_{n=1}^{N} e^{-mn\tau}\tilde{z}_\varphi^T(t)T\tilde{z}_\varphi(t) - k\eta(t) - v^T(t)I_2v(t)
\end{aligned} \tag{19}$$

Combining Equation (19), and applying Young's inequality:

$$2\tilde{x}^T(t)P\tilde{D}\sum_{n=1}^{N}\tilde{\tilde{z}}_\varphi(t-n\tau) \le 3\tilde{x}^T(t)P\tilde{D}\tilde{D}^TP^T\tilde{x}(t) + \sum_{n=1}^{N}\tilde{z}_\varphi^T(t-n\tau)\tilde{z}_\varphi(t-n\tau) \tag{20}$$

Combining equation (19) and equation(20), it can be derived that:

$$\begin{aligned}
&\dot{W}(\tilde{x}(t)) + \tilde{z}^T(t)\tilde{z}(t) - \beta^2\tilde{\xi}^T(t)\tilde{\xi}(t) \\
&\le \bar{x}^T(t)\Gamma\bar{x}(t) - k\eta(t) - \sum_{n=1}^{N}\tilde{z}_\varphi^T(t-n\tau)\left((T-I_3)\,e^{-m(t-n\tau)} - I_{2\times 2}\right)\tilde{z}_\varphi(t-n\tau) + 2\tilde{x}^T(t)PL^f,
\end{aligned} \tag{21}$$

where

$$\bar{x}(t) = [\tilde{x}_\varphi^T(t)\ \ \tilde{\xi}^T(t)\ \ v(t)^T]^T,$$

$$\Gamma = \begin{bmatrix} \Lambda & P\tilde{B} & P\tilde{E} \\ * & -\beta^2 I & 0 \\ * & * & -I_2 \end{bmatrix}.$$

Assuming the formulas $T - I_3 > I$ and $L^f \le 0$ hold.
When $\tilde{\xi}^T(t) \equiv 0$, one can infer that

$$\dot{W}(\tilde{x}_\varphi(t)) \le 0 \tag{22}$$

When $\tilde{\xi}^T(t) \ne 0$, for $\forall\tilde{\xi}^T(t) \in L_2(0,\infty)$, integrating (21), we can obtain

$$\int_0^t z^T(\tau)z(\tau)\,d\tau - \beta^2\int_0^t \tilde{\xi}^T(\tau)\tilde{\xi}(\tau)\,d\tau \le W(\tilde{x}(0)) - W(\tilde{x}(t)) \le 0 \tag{23}$$

Let $t \to \infty$, the L_2-gain performance of the AS (6) is proved. □

Then, the following theorem is provided to cope with the coupling terms Λ in Theorem 1 and to solve the disturbance observer (8) and controller (11).

Theorem 2. *Let constants $\sigma > 0$ be given. Assume that there exist positive definite strictly symmetric matrices P_1, P_2 and a matrix L such that the constraints*

$$\begin{bmatrix} \Pi_{11} & GC & E & 0 & GL & P_1^{-1}H \\ * & \Delta_{22} & P_2\Lambda E & P_2 B & 0 & 0 \\ * & * & -\beta^2 I & 0 & 0 & 0 \\ * & * & * & -\beta^2 I & 0 & 0 \\ * & * & * & * & -I_2 & 0 \\ * & * & * & * & * & \Delta_{66} \end{bmatrix} < 0, \tag{24}$$

hold, where

$$\Pi_{11} = P_1^{-1}(F+GL)^T + (F+GL)P_1^{-1} + P_1^{-1}\sigma I_{11} P_1^{-1},$$
$$\Delta_{66} = -\frac{1}{\left(\sum_{n=1}^{N} e^{-mn\tau} + 1\right)} I,$$

then, the disturbance observer (8), DMETM (9) and controller (11) constitute the H_∞ ADDMET control scheme of the augmented system (14). Besides, the sliding window disturbance observer gain (8) and controller gain (11) are computed by LMI.

Proof. First of all, we display that the constraints (16) and (24) are equivalent. By virtue of Schur complement lemma

$$\begin{bmatrix} \Xi^{11} & P\tilde{B} & P\tilde{E} & \tilde{H}^T \\ * & -\beta^2 I & 0 & 0 \\ * & * & -I_2 & 0 \\ * & * & * & \Delta_{66} \end{bmatrix} < 0$$

$$\Xi^{11} = P\tilde{A} + \tilde{A}^T P + \sigma I_1,$$

Replacing the specific forms of $\tilde{A}$, $\tilde{B}$, $\tilde{D}$, $\tilde{E}$ and $\tilde{H}$ into (16) develops

$$\begin{bmatrix} \Delta_{11} & P_1 GC & P_1 E & 0 & P_1 GL & H^T \\ * & \Delta_{22} & P_2\Lambda E & P_2 B & 0 & 0 \\ * & * & -\beta^2 I & 0 & 0 & 0 \\ * & * & * & -\beta^2 I & 0 & 0 \\ * & * & * & * & -I_2 & 0 \\ * & * & * & * & * & \Delta_{66} \end{bmatrix} < 0$$

with

$$\Delta_{11} = P_1(F+GL) + (F+GL)^T P_1 + \sigma I_{11},$$
$$\Delta_{22} = P_2(A+\Lambda GC) + (A+\Lambda GC)^T P_2 + \sigma I_{12},$$

Multiplying two sides of the above restrain by $diag\{P_1^{-1}, I, I, I, I, I, I\}$, one can conclude (24). □

Next, let us exhibit that the Zeno phenomenon will not be induced by the DMETM (9).

Theorem 3. *Consider the DMETM defined in (9) and the internal dynamic variable $\eta(t)$ governed by (10). Suppose that the closed-loop system satisfies the LMIs given in Theorem 1 so that the Lyapunov functional $W(t)$ in (17) guarantees the boundedness of $\tilde{x}(t)$, $\eta(t)$, $\tilde{\xi}(t)$, and $\tilde{z}_\varphi(t)$ over any finite interval. Furthermore, assume that the augmented dynamics (14) satisfy the following growth condition: there exists a constant $L > 0$ such that*

$$\|\dot{x}_\varphi(t)\| \le L\big(1 + \|\tilde{x}(t)\| + \|\tilde{\xi}(t)\|\big), \quad \forall t \ge 0. \tag{25}$$

Then the proposed DMETM is free of Zeno behavior. That is, there exists a constant $\tau_{\min} > 0$ such that

$$t_{\mathfrak{s}+1} - t_{\mathfrak{s}} \ge \tau_{\min} > 0, \qquad \forall \mathfrak{s} \in \mathfrak{N}.$$

Proof. The triggered function is defined as

$$\Phi(t) = \eta(t) + \iota\Big(\sigma\tilde{x}^T(t)I_1\tilde{x}(t) - v^T(t)I_2v(t)\Big), \tag{26}$$

where $v(t) = x_\varphi(t_\mathfrak{s}) - x_\varphi(t)$.

Differentiating $\Phi(t)$ along system trajectories yields

$$\dot{\Phi}(t) = \dot{\eta}(t) + \iota\frac{d}{dt}\left(\sigma\tilde{x}^T I_1\tilde{x} - v^T I_2 v\right). \tag{27}$$

From (10), it follows that

$$|\dot{\eta}(t)| \le \kappa|\eta(t)| + \iota\Big|\sigma\tilde{x}^T I_1\tilde{x} - v^T I_2 v\Big| + m\sum_{n=1}^{N} e^{-m(t-n\tau)}\Big\|\tilde{z}_\varphi(t-n\tau)\Big\|^2\|I_3\|.$$

Since Theorem 1 guarantees that $\tilde{x}(t)$, $\tilde{\xi}(t)$, $\eta(t)$ and $\tilde{z}_\varphi(t)$ remain bounded, there exist constants $\overline{X}$, $\overline{\Xi}$, and $\overline{\eta}$ such that

$$|\dot{\eta}(t)| \le \kappa\overline{\eta} + \iota\sigma\|I_1\|\overline{X}^2 + \iota\|I_2\|\|v(t)\|^2 + R_{\max},$$

where $R_{\max}$ collects the bounded sliding-window terms.

Note that

$$\frac{d}{dt}(\sigma\tilde{x}^T I_1\tilde{x}) = 2\sigma\tilde{x}^T I_1\dot{\tilde{x}},$$

and

$$\frac{d}{dt}(v^T I_2 v) = 2v^T I_2\dot{v} = -2v^T I_2\dot{x}_\varphi.$$

Using the growth condition (25) gives

$$\left|\tfrac{d}{dt}(\sigma\tilde{x}^T I_1\tilde{x} - v^T I_2 v)\right| \le 2\sigma\|I_1\|\overline{X}B_x + 2\|I_2\|\|v(t)\|B_x,$$

where

$$B_x = L(1 + \overline{X} + \overline{\Xi}).$$

Combining the above inequalities yields

$$|\dot{\Phi}(t)| \le C_0 + C_1\|v(t)\| + C_2\|v(t)\|^2,$$

where

$$\begin{aligned} C_0 &= \kappa\overline{\eta} + \iota\sigma\|I_1\|\overline{X}^2 + R_{\max} + 2\iota\sigma\|I_1\|\overline{X}B_x,\\ C_1 &= 2\iota\|I_2\|B_x,\\ C_2 &= \iota\|I_2\|. \end{aligned}$$

Since

$$v(t) = \int_{t_\mathfrak{s}}^{t} -\dot{x}_\varphi(\tau)\,d\tau,$$

one obtains

$$\|v(t)\| \le B_x(t - t_\mathfrak{s}).$$

Hence for any sufficiently small interval $[t_\mathfrak{s}, t_\mathfrak{s} + \delta]$, there exists a constant $V_{\max}$ such that $\|v(t)\| \le V_{\max}$. Therefore,

$$|\dot{\Phi}(t)| \le M,$$

for some constant $M > 0$.

At each triggered instant $t_\mathfrak{s}$, $\Phi(t_\mathfrak{s}) = 0$ and $v(t_\mathfrak{s}) = 0$. Hence

$$\eta(t_\mathfrak{s}) = -\iota\sigma\tilde{x}^T(t_\mathfrak{s})I_1\tilde{x}(t_\mathfrak{s}).$$

Because $I_1 \succ 0$ and $\tilde{x}(t)$ is bounded, there exists $\underline{\Psi} > 0$ such that

$$\Psi(t_\mathfrak{s}) = \iota\sigma\tilde{x}^T(t_\mathfrak{s})I_1\tilde{x}(t_\mathfrak{s}) \ge \underline{\Psi}.$$

Meanwhile, $\eta(t)$ is bounded from below by the Lyapunov functional, $\eta(t) \geq \underline{\eta}$.

Hence the triggered function must decrease by at least

$$\Delta^* = \underline{\Psi} + \underline{\eta} > 0$$

before the next event occurs.

Since $|\dot{\Phi}(t)| \leq M$, it follows that

$$\Delta^* \leq \int_{t_\mathfrak{s}}^{t_{\mathfrak{s}+1}} |\dot{\Phi}(t)| dt \leq M(t_{\mathfrak{s}+1} - t_\mathfrak{s}).$$

Therefore,

$$t_{\mathfrak{s}+1} - t_\mathfrak{s} \geq \tau_{\min} = \frac{\Delta^*}{M} > 0.$$

This shows that infinitely many triggered instants cannot accumulate within a finite time interval. Therefore, Zeno behavior is strictly excluded. □

4. Verification

In this section, a simulation for the RMS (4) is used to show the superiority and effectiveness of the H_∞ ADDMET control method.

The data of the AS (6) with (5) are listed as

$$F = \begin{bmatrix} -2.9378 & 1.0937 \\ 0.4149 & -3.4793 \end{bmatrix}, G = \begin{bmatrix} -1 \\ -2 \end{bmatrix},$$
$$H = \begin{bmatrix} -0.0047 & -0.0172 \\ 0.49 & -3.4793 \end{bmatrix}, E = \begin{bmatrix} -0.5 \\ -0.3 \end{bmatrix},$$

$$b = \begin{bmatrix} 0.002 \\ -0.001 \end{bmatrix}, A = \begin{bmatrix} 0 & 1 \\ -3 & 0 \end{bmatrix}, B = \begin{bmatrix} 0.01 \\ 0.02 \end{bmatrix}, C = \begin{bmatrix} 2 & 1 \end{bmatrix}.$$

The control task is to realize the speed regulation of the RMS (4) formulated by the AS (6). To demonstrate the effectiveness of the proposed method, the stability and convergence performance of the developed disturbance observer are evaluated. The results are obtained based on the proposed H_∞ ADDMET control scheme. Furthermore, in terms of communication resource conservation, a comparison has been made between DMET [26] and DET [28,29].

Letting $x_\varphi(t) = x(t) - x^\varphi$, the desired EP is $x^\varphi = [-0.2694\ -0.0268]^T \times 10^{-3}$ associated with $\varphi = [0\ 0.7]^T$. For (24) , we obtain the L_2-gain level $\beta = 1$. The gains of disturbance observer (8) and controller (11) are calculated as

$$\Lambda = \begin{bmatrix} 8.1178 & -18.5678 \\ -18.5678 & 61.9500 \end{bmatrix},$$
$$L = \begin{bmatrix} -28.4467 & 292.4693 \end{bmatrix},$$

The experimental results are illustrated in Figures 1–4. Figure 1 depicts the disturbance $\xi_1(t)$, its estimation $\hat{\xi}_1(t)$, and the estimation error $e(t) = \xi_1(t) - \hat{\xi}_1(t)$. It can be observed that the proposed observer accurately tracks the disturbance generated by the exo-system (5).

Figures 2 and 3 further present the evolution of the system states and control inputs, including joint state responses and control torque signals. Under the proposed control scheme, all state variables converge smoothly to the equilibrium point without noticeable overshoot, indicating satisfactory transient and steady-state performance. Meanwhile, the control inputs remain bounded and smooth, without undesirable oscillations, even under event-triggered updates.

Figure 4 shows the ET intervals $\{t_{\mathfrak{s}+1} - t_\mathfrak{s}\}$, and indicates that no Zeno phenomenon occurs. Note that DMET features fewer triggers and longer trigger interval compared to DET. Obviously, from Figure 4, we can observe that compared to DET, DMET demonstrates a more significant saving in communication resource. DMET conserves more communication resources compared to DET and ensures that the system state ultimately converges to zero. Consequently, one can assert that the constructed H_∞ ADDMET control scheme effectively achieves the speed adjustment of the AS (6).

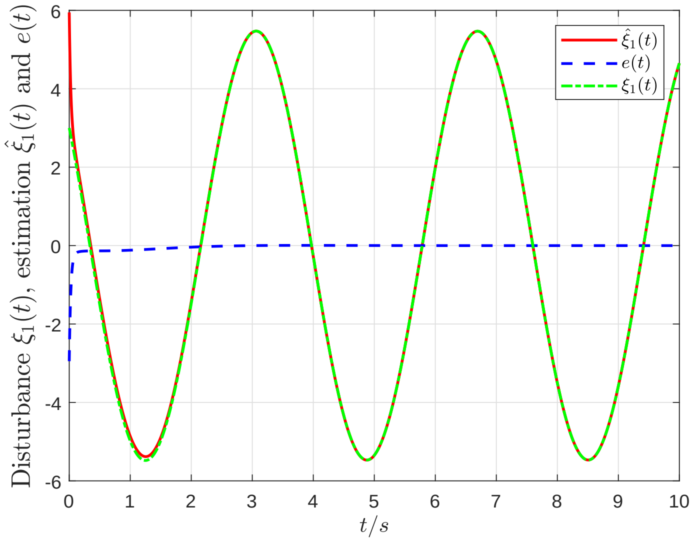

Figure 1. Disturbance $\xi_1(t)$, estimation $\hat{\xi}_1(t)$ and estimation error $e(t)$.

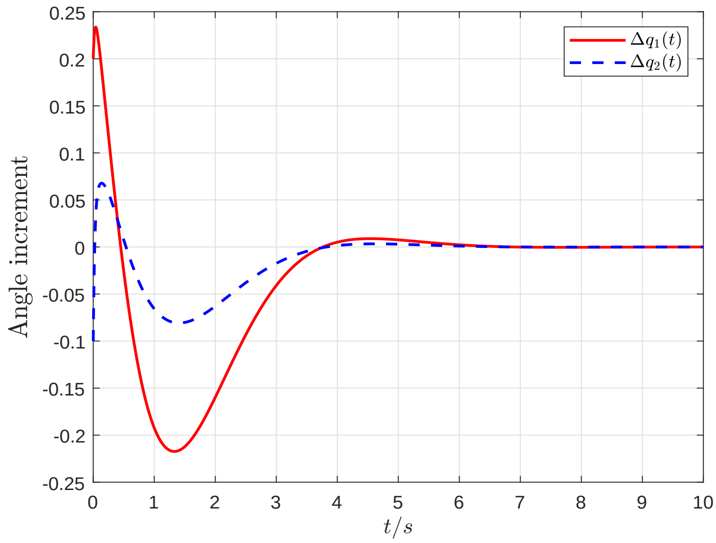

Figure 2. Joint 1 angle increment $\Delta q_1(t)$ and Joint 2 angle increment $\Delta q_2(t)$.

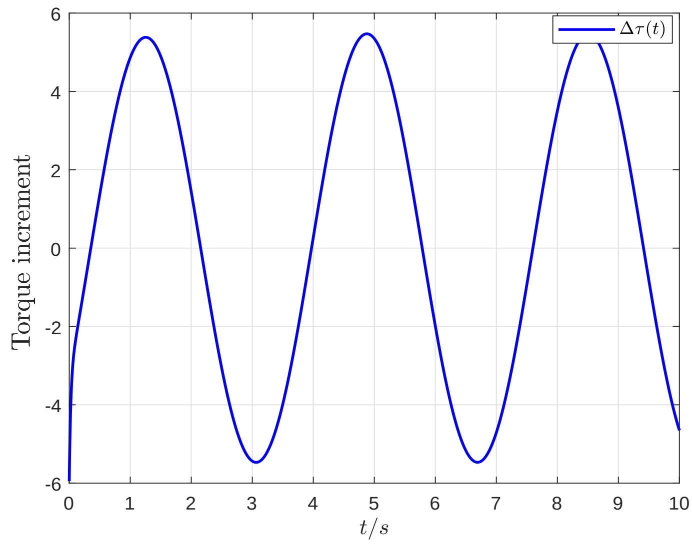

Figure 3. Torque increment $\Delta\tau(t)$.

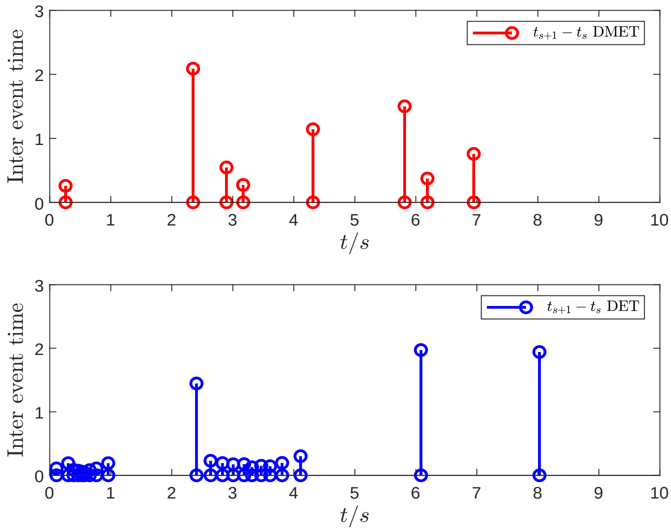

Figure 4. ET intervals $\{t_{s+1} - t_s\}$.

5. Conclusions

In this paper, the H_∞ ADDMET control problem for RMS subject to both modeled and unmodeled disturbances has been investigated. Firstly, an affine model has been established to characterize performance degradation and complex operating conditions of RMS. Then, a disturbance observer has been developed to estimate and compensate for modeling errors, uncertainties, and external disturbances. Subsequently, a DMETM has been constructed to effectively reduce communication burden between the RMS and the controller while excluding Zeno behavior.

Based on the proposed observer and DMETM, an H_∞ ADDMET control scheme has been designed, and corresponding sufficient conditions have been derived to guarantee the desired H_∞ performance for the affine system.

Finally, simulation results have verified the effectiveness and feasibility of the proposed control strategy for RMSs under the affine framework. A particularly promising direction is to incorporate fractional-order dynamics and stochastic differential characteristics into the affine modeling framework. This extension would allow for a more precise characterization of systems with memory effects and random perturbations [31–34].

Author Contributions

P.Z.: conceptualization, methodology, writing—original draft preparation; Y.Z.: supervision, conceptualization, writing—reviewing and editing; C.X.: data curation, validation, formal analysis; C.Z.: investigation, visualization. All authors have read and agreed to the published version of the manuscript.

Funding

This work was supported in part by the National Natural Science Foundation of China under Grant 62373072, 62073054, and 62003070; The Zhejiang Pioneer Plan Project (No. 2025C01050); and the China Postdoctoral Science Foundation with grant number 2024M764265.

Institutional Review Board Statement

Not applicable.

Informed Consent Statement

Not applicable.

Data Availability Statement

The authors confirm that the data supporting the findings of this study are available within the article.

Conflicts of Interest

The authors declare no conflict of interest.

Use of AI and AI-Assisted Technologies

No AI tools were utilized for this paper.

References

1. Khan, G.D. Adaptive neural network control framework for industrial robot manipulators. *IEEE Access* **2024**, *12*, 63477–63483.
2. Ueda, J.; Kwon, H. Perfectly undetectable reflection and scaling false data injection attacks via affine transformation on mobile robot trajectory tracking control. *IEEE Trans. Robot.* **2025**, *41*, 6403–6418.
3. Tang, J.; Li, J.; Zhou, J.; et al. Prescribed-time affine formation control for nonholonomic constrained robots. In Proceedings of the 2025 4th Conference on Fully Actuated System Theory and Applications (FASTA), Nanjing, China, 4–6 July 2025; pp. 712–717.
4. Nubert, J.; Kohler, J.; Berenz, V.; et al. Safe and fast tracking on a robot manipulator: Robust MPC and neural network control. *IEEE Robot. Autom. Lett.* **2020**, *5*, 3050–3057.
5. Cisneros, P.S.G.; Sridharan, A.; Werner, H. Constrained predictive control of a robotic manipulator using quasi-LPV representations. *IFAC-PapersOnLine* **2018**, *51*, 118–123.
6. San-Miguel, A.; Puig, V.; Alenya, G. Disturbance observer-based LPV feedback control of a N-DoF robotic manipulator including compliance through gain shifting. *Control Eng. Pract.* **2021**, *115*, 104887.
7. Zhang, C.; Wu, Y.Q. P-Rob six-degree-of-freedom robot manipulator dynamics modeling and anti-disturbance control. *IEEE Access* **2021**, *9*, 141403–141420.
8. Xie, H.H.; Dai, L.; Lu, Y.C.; et al. Disturbance rejection MPC framework for input-affine nonlinear systems. *IEEE Trans. Autom. Control* **2022**, *67*, 6595–6610.
9. Cheng, J.; Wu, Y.Y.; Wu, Z.G.; et al. Nonstationary filtering for fuzzy Markov switching affine systems with quantization effects and deception attacks. *IEEE Trans. Syst. Man Cybern. Syst.* **2022**, *52*, 6545–6554.
10. Wang, M.; Qiu, J.B.; Yan, H.C.; et al. Data-driven control for discrete-time piecewise affine systems. *Automatica* **2023**, *155*, 111168.
11. Li, Z.Y.; Zhao, J. A Zeno-free event-triggered control strategy for asymptotic stabilization of switched affine systems. *IEEE Trans. Autom. Control* **2022**, *67*, 5509–5516.
12. Martinelli, A.; Gargiani, M.; Draskovic, M.; et al. Data-driven optimal control of affine systems: A linear programming perspective. *IEEE Control Syst. Lett.* **2022**, *6*, 3092–3097.
13. Chang, W.M.; Li, Y.M.; Tong, S.C. Adaptive fuzzy backstepping tracking control for flexible robotic manipulator. *IEEE/CAA J. Autom. Sin.* **2021**, *8*, 1923–1930.
14. Xu, X.Z.; Zhu, Y.Z.; Wu, F.; et al. Sampled-data control for buck-boost converter using a switched affine systems approach. *IEEE Trans. Circuits Syst. I Regul. Pap.* **2024**, *71*, 3380–3389.
15. Liao, F.; Zhu, Y.Z.; He, X.; et al. Fault estimation of continuous-time switched affine systems with actuator faults under dwell time constraint. *Int. J. Robust Nonlinear Control* **2024**, *34*, 1417–1432.
16. Hashemi, S.M.; Abbas, H.S.; Werner, H. Low-complexity linear parameter-varying modeling and control of a robotic manipulator. *Control Eng. Pract.* **2012**, *20*, 248–257.
17. Pan, M.X.; Xu, Y.; Gu, B.B.; et al. Fuzzy-set theoretic control design for aircraft engine hardware-in-the-loop testing: Mismatched uncertainty and optimality. *IEEE Trans. Ind. Electron.* **2022**, *69*, 7223–7233.
18. Li, P.; Zhao, X.D.; Qin, H.Q. Event-triggered model predictive control for aero-engine transient-state tracking problems. *J. Aerosp. Inf. Syst.* **2023**, *20*, 229–239.
19. Xie, J.; Yang, D.; Zhao, J. Composite anti-disturbance model reference adaptive control for switched systems. *Inf. Sci.* **2019**, *485*, 71–86.
20. Zhang, B.; Zhang, T.; Xi, Z.S.; et al. Estimate-based dynamic memory-event-triggered control for nonlinear networked control systems subject to hybrid attacks. *Mathematics* **2025**, *13*, 2829.
21. Yao, X.M.; Guo, L. Composite anti-disturbance control for Markovian jump nonlinear systems via disturbance observer. *Automatica* **2013**, *49*, 2538–2545.
22. Xu, G.Y.; Yin, L.P. Event-triggered adaptive sliding mode control for robotic arms with predefined-time convergence. In Proceedings of the 2025 IEEE/ASME International Conference on Advanced Intelligent Mechatronics (AIM), Hangzhou, China, 14–18 July 2025.
23. Yan, T.; Zhao, X.; Zhang, Y.; et al. Adaptive predefined-time event-triggered consensus tracking control for robotic multi-agent system. *Int. J. Intell. Control Syst.* **2025**, *30*, 16–26.
24. Chu, C.Y.; He, Y.Q. A unified neural event-triggered control approach of high-order switched uncertain systems with time-varying state constraints. *Robot. Intell. Autom.* **2026**, *46*, 290–302.
25. Li, P.; Zhao, X.D.; Qin, H.; et al. Dynamic event-triggered finite-time H_∞ tracking control of switched LPV aero-engine models. *IEEE Trans. Circuits Syst. II Express Briefs* **2022**, *69*, 1114–1118.

26. Hou, Q.H.; Dong, J.X. Finite-time membership function-dependent H_∞ control for T-S fuzzy systems via a dynamic memory event-triggered mechanism. *IEEE Trans. Fuzzy Syst.* **2023**, *31*, 4075–4084.
27. Wang, T.Y.; Chen, Y.D. Event-triggered control of flexible manipulator constraint system modeled by PDE. *Math. Biosci. Eng.* **2023**, *20*, 10043–10062.
28. Ma, Y.K.; Tang, W.T.; Fei, Z.Y.; et al. Dynamic event-triggered sensor fault interval estimation and accommodation for aeroengine. *IEEE Trans. Ind. Electron.* **2023**, *71*, 4191–4200.
29. Gao, Y.X.; Zhao, Y.; Sang, H.; et al. Dynamic event-triggered-based anti-disturbance control for uncertain LPV systems. *Int. J. Robust Nonlinear Control* **2023**, *33*, 11275–11290.
30. Duan, R.; Yu, H. *LMIs in Control Systems: Analysis, Design and Applications*; CRC Press: Boca Raton, FL, USA, 2013.
31. Dhayal, R.; Gómez-Aguilar, J.F. Successive approximation and stability analysis of Hilfer fractional stochastic differential systems with application to circuits. *Int. J. Syst. Sci.* **2026**, *57*, 361–371.
32. Vijayakumar, V.; Nisar, K.S.; Chalishajar, D.; et al. A note on approximate controllability of fractional semilinear integrodifferential control systems via resolvent operators. *Fractal Fract.* **2022**, *6*, 73.
33. Elgroud, N.; Dhayal, R.; Malik, M. Approximate controllability of damped impulsive fractional stochastic differential systems driven by Lévy process. *Stoch. Dyn.* **2026**, *26*, 2650001.
34. Dhanush, A.; Vijayakumar, V. A class of higher-order fractional stochastic differential inclusions and feedback control results. *Appl. Anal.* **2026**, 1–28. https://doi.org/10.1080/00036811.2026.2659840.